

Preliminary analysis of the RTK positioning using Android GNSS Raw Measurements and Application Feasibility for the Trajectory mapping using UAV's

Himanshu Sharma, Andreas Schütz, Thomas Pany
Institute of Space Technology and Space Applications (ISTA), Faculty of Aerospace Engineering,
Universität der Bundeswehr München, 85577 Neubiberg, Germany

BIOGRAPHY (IES)

Himanshu Sharma is a Research Associate at the Institute of Space Technology and Space Applications (ISTA). He received his Bachelors in Technology (B. Tech) degree in the field of Electronics and Communication from the Maharishi Dayanand University, Rohtak, India. He accomplished his Masters in Science (M.Sc.) in the field of Communications and Signal Processing from Technical University of Ilmenau, Thuringia, Germany. His research interests are precise positioning and Signal Processing. Currently, He is involved in the project focused on RTK positioning using the mobile phone GNSS Raw Data.

Andreas Schütz is a Research Associate at the Institute of Space Technology and Space Applications (ISTA). He received his Bachelors and Masters in the field of Geodesy and Geoinformation from Technical University Munich, Germany. His research focuses on Precise GNSS Positioning and Receiver Technology, as well as Integrity and Sensor Fusion. He is currently involved in a project regarding RTK/IMU coupling on smartphones and PPP IMU coupling for automotive applications.

Prof. Thomas Pany is with the Universität der Bundeswehr München where he leads the satellite navigation unit LRT 9.2 of the Institute of Space Technology and Space Applications (ISTA). He teaches navigation focusing on GNSS, inertial sensors and aerospace applications. His unit investigates signal design, GNSS transceivers and high-integrity multi-sensor navigation (inertial, LiDAR) and is also developing a modular UAV-based GNSS test bed. He has a PhD from the Graz University of Technology and used to work for IFEN GmbH where he created the SX3 software receiver. He authored around 200 publications including one monography and received five best presentation awards from the US institute of navigation.

ABSTRACT

With the release of Android N, Google announced the availability of GNSS Raw data from the mobile phone. This opens up to the broader prospective for research, analysis and enhancement of the positioning quality in mobile phones. With increasing applications based upon augmented reality, e-banking, e-health, etc., there is a rapid increase in the demand for precise positioning using the existing architecture of mobile devices.

But, the quality of carrier phase raw data is not adequate for the substantial RTK (precise positioning). Artifacts in smartphone GNSS antenna, environmental degradation and cycle slips are few of the major issues to be addressed for reliable carrier phase positioning in the smartphone. The code range residual for kinematic and static measurement setup are very noisy in comparison to carrier phase residual. This results in invalid positioning solution with wrong ambiguity fixing. Doppler smoothed code pseudorange (Kalman Filter) shows a considerable improvement in the positioning accuracy as compared to standard SPP solution. The RTK positioning is feasible with the raw GNSS data from the smartphone, but only float solutions are reliable. The position error due to gyroscope bias in x and y axis is 0.0036 m and 0.0032 m respectively and thus, can be used for small cycle slips detection and corrections.

INTRODUCTION

GNSS positioning has always been the most reliable and accurate method for navigation and positioning. But, since the evolution of GNSS positioning system, there has always been a tradeoff between the accuracy and the cost of the receiver. Survey grade receivers which demands centimeters level accuracy cost thousands of euros. Whereas, GNSS receivers in mobile phone, cost comparatively less. But, provide user with several meters accuracy. With rapidly increasing demand of higher position accuracy, a promising solution is a must.

GNSS is the must have feature for the smartphone with the estimated 86 percent of GNSS receivers embedded in the mobile phones. Although the incumbent GPS chip has high sensitivity, the integrated result cannot performance in the low signal condition. The quality of GNSS antenna and the interference caused in the GNSS band within the mobile phone are the two major reasons. The code range based positioning technique incorporated in the mobile phone is highly influenced by noise. The carrier phase range measurement technique based on estimation of number carrier cycles, is much more precise but, require a continuous tracking of the satellites even in the degraded environment. "Duty cycling" in the mobile phone provide mobile user with extended battery life but, decay the chances of carrier phase ranging in the mobile phone due to the cycle slips. Additionally, effects such as multipath and degradation due to atmosphere are the major contributors in limiting the positioning accuracy in the mobile phones.

With the availability of GNSS raw data from the mobile phone, there is a growing interest in analyzing the quality of raw data and its feasibility for precise positioning. The research work focused in the paper is highly dedicated in analyzing the quality of GNSS raw data and its RTK performance analysis.

The approach presented in the paper showcase the quality of GNSS raw data, standard single point positioning solution, Doppler smoothed single point positioning solution and finally RTK positioning solution. The paper demonstrates the quality of RTK solutions in post-processing. In order to analyze the quality, kinematic and retransmission setups were performed. The analysis is based upon single (L1) frequency using GPS constellation only.

MEASUREMENT SETUP

The raw GNSS data logging for the analysis was performed using the GNSS/INS logger developed at the Institute of Space Technology and Space Applications (ISTA). The ISTA logger is an android based application capable of logging GNSS and INS (Accelerometer, Gyroscope and Magnetometer) data from the embedded sensors in the mobile phones. In the first phase of data logging, mobile phone (Samsung S8) was mounted on the Drone (see figure). The raw GNSS data was logged during the drone flight for approx. 15 minutes. The reference GNSS data during the setup was logged using the Trimble R10 receiver with in the range of approx. 200 meter from the drone (S8 mounted). Additionally, to analyze the accuracy of RTK solution using the S8 raw data, LEICA MS60 multistation was placed to acquire the reference trajectory.

In the second phase of data logging, a retransmission setup was performed. A roof top antenna was used to provide input to Trimble NetR9 (reference receiver for RTK) and Samsung S8. The input signal to Samsung S8 was amplified and retransmitted using a patch antenna. The idea behind this setup to compensate for the poor signal reception of the GNSS antenna embedded in the mobile phone.

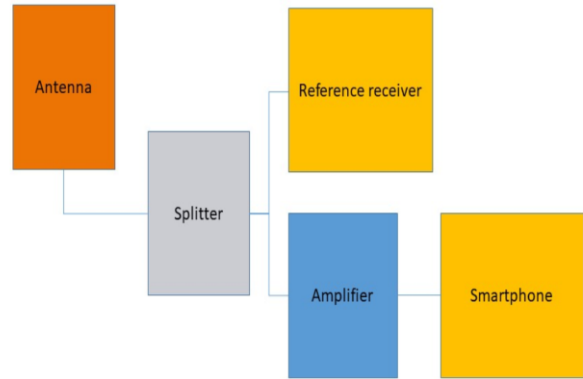


Figure 1: (Left) Samsung S8 mounted on the Drone (Right) Retransmission setup

The logged raw GNSS data is then processed with the MuSNAT receiver Software. The MuSNAT receiver has an integrated navigation module capable of performing single point positioning and RTK positioning. The navigation module has an integrated RTKLib for performing RTK positioning.

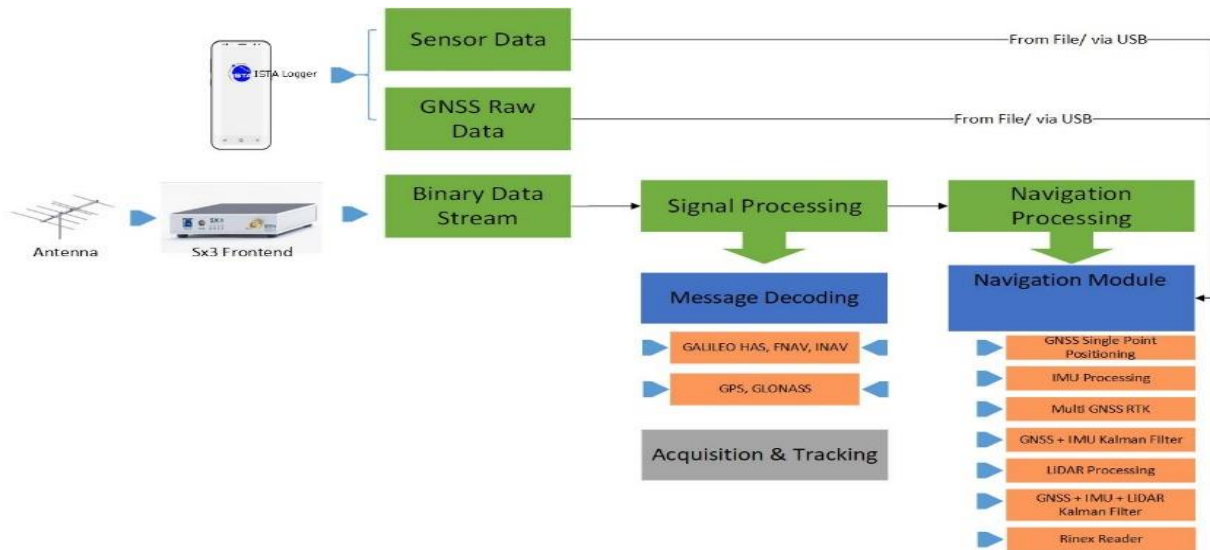


Figure 2: MuSNAT Receiver Software flow

For further analysis of GNSS raw data, LMSOFT software module was used for performing RTK positioning. The detailed setup parameter has been explained in the tables below.

	SPP		RTK
	KalmanFilter		RTKLIB 2.4.3
Baseline	N/A	N/A	Small baseline (< 200 meter)
Measurement Noise	20 m, 10 cm/s	20 m	
Process Noise	Clk: 100 m, ...	N/A	
Ambiguity Threshold	N/A	N/A	3
Ambiguity Resolution Technique	N/A	N/A	LAMBDA, Continuous
Constellation Type	GPS only	GPS only	GPS only
Frequency	L1 only	L1 only	L1 only
Rover (mobile)	Samsung S8	Samsung S8	Samsung S8
Reference	N/A	N/A	Trimble R10
Atmospheric Correction model	No	No	No
Solution Validation (chi-squared)	N/A	N/A	Deactivated
Observable Type	Code pseudoranges plus Doppler	Code pseudorange	Code pseudorange plus carrier phase

	SPP		RTK
	With KF	Without KF	RTKLIB, LMSOFT (float RTK)
Baseline	N/A	N/A	Zero baseline
Measurement Noise	20 m, 10 cm/s	20 m	
Process Noise	Clk: 100 m	N/A	Dynamic
Ambiguity Threshold	N/A	N/A	3
Ambiguity Resolution Technique	N/A	N/A	LAMBDA, Continuous
Constellation Type	GPS only	GPS only	GPS only
Frequency	L1 only	L1 only	L1 only
Rover (mobile)	Samsung S8	Samsung S8	Samsung S8
Reference	N/A	N/A	Trimble NetR9
Atmospheric Correction model	No	No	No
Solution Validation (chi-squared)	N/A	N/A	Deactivated
Observable Type	Code pseudoranges plus Doppler	Code pseudorange	Code pseudorange plus carrier phase

Figure 3: Setup Description (Left) Drone Flight Analysis (Right) Retransmission Analysis

DRONE FLIGHT ANALYSIS

The C/N0 for the satellites recoded during the Drone flight with Samsung S8 shows at least five satellite with C/N0 greater than 35 dB-Hz throughout the flight duration. The threshold C/No used for SPP and RTK was 30 dB-Hz.

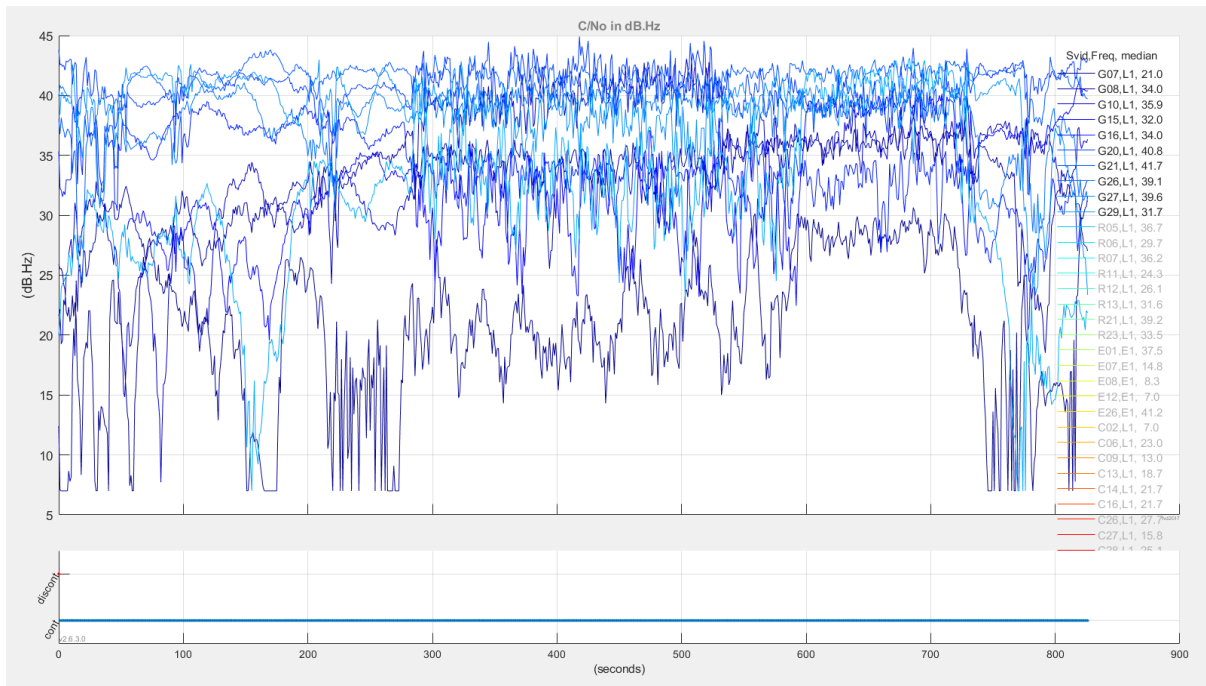


Figure 4: C/N0 plot for S8 during Drone Flight

The Kinematic standard SPP solution using Samsung S8 during the drone flight is depicted in the Figure 5. The results demonstrate high fluctuations in the longitude values in comparison to reference trajectory from LEICA system.

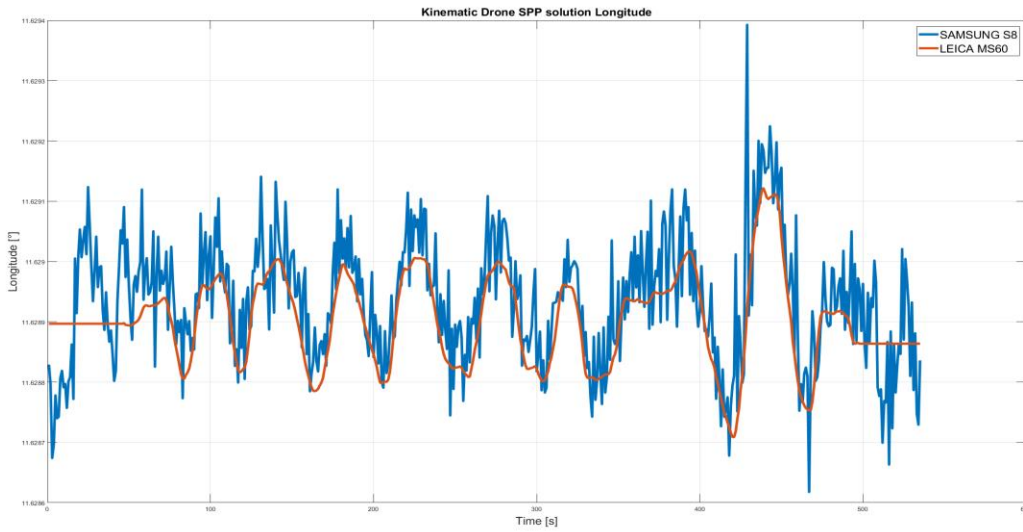


Figure 5: Kinematic Drone SPP Solution Longitude

In another scenario for SPP, a Kalman filter based SPP solution was produced using the similar raw GNSS data. The positioning solution has improved significantly. The error in position with reference to the reference trajectory (LEICA) lies within the range of 10 meter as shown in the Figure 6.

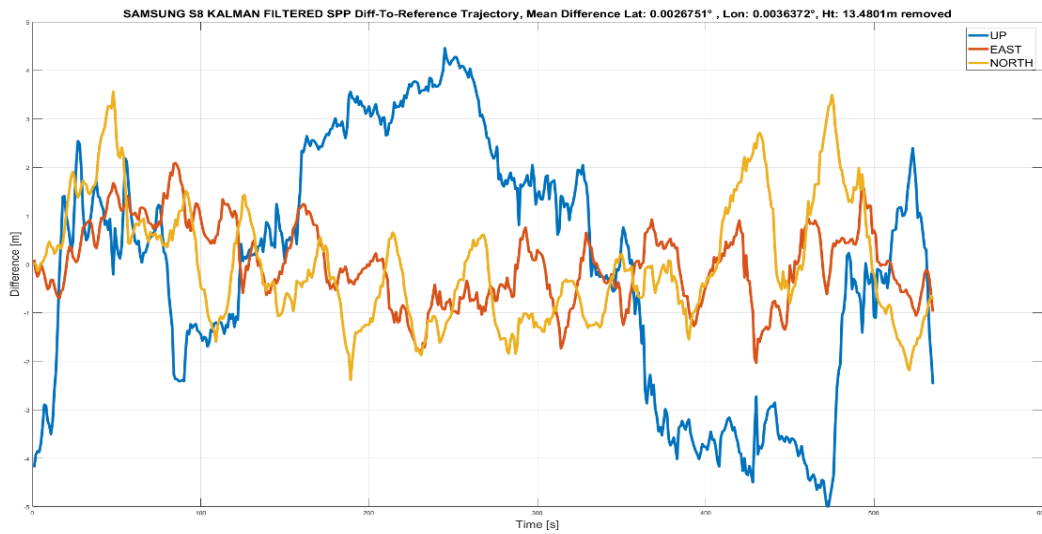


Figure 6: Samsung S8 Kalman Filtered SPP solution

Figure 7 shows height accuracy for SPP solution with and without Kalman filter processing w.r.t reference trajectory. A significant improvement in height accuracy is attained by using Kalman filtered SPP solution in comparison to standard SPP solution.

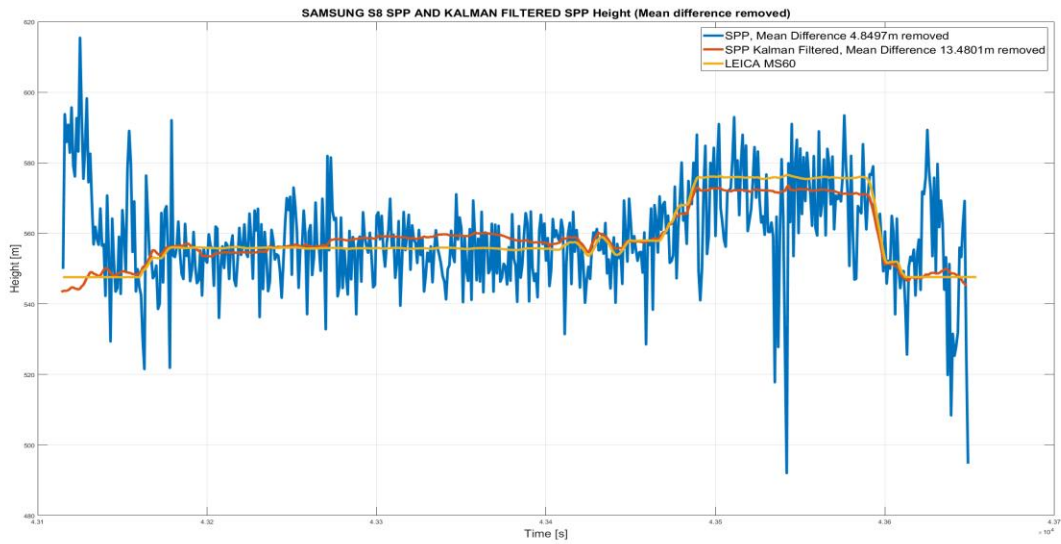


Figure 7: Samsung S8 Kalman Filtered SPP solution (Height)

The Kalman filtered SPP code RMS value calculated with predicted minus observed pseudorange. The plot shown in the Figure 8 shows an interesting feature where code RMS value peak jumps after every few epochs. This might be the filter tuning issue or an artifact from the GNSS chipset. The Doppler RMS value was investigated. Figure 9 illustrate that the predicted minus observed Doppler value is higher when the drone is flying due to constraint filtering. The higher Doppler residual in turn provide better RTK positioning float solution as shown in the Figure 10.

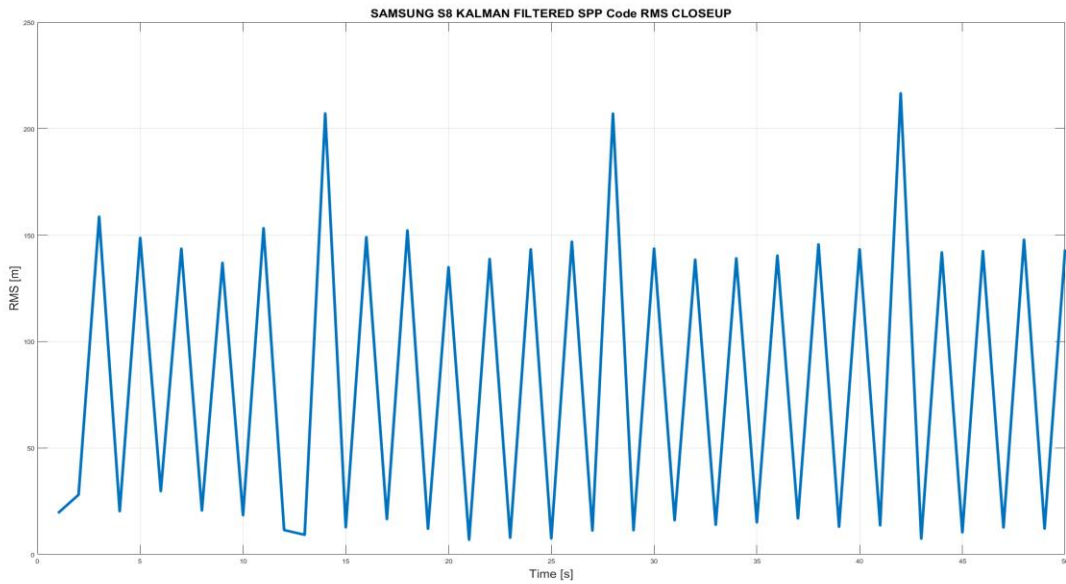


Figure 8: Samsung S8 Kalman Filtered Code RMS

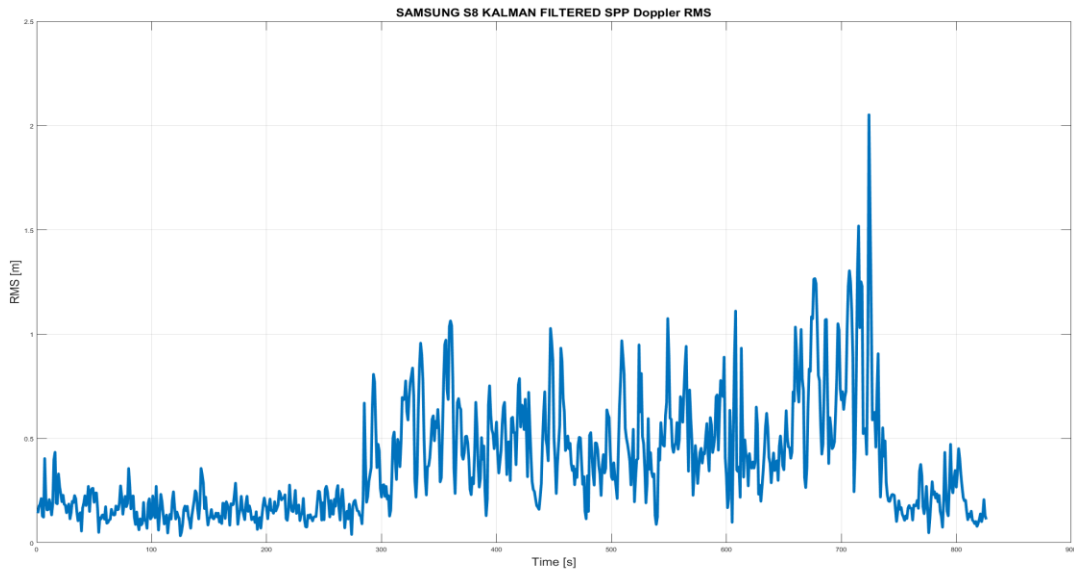


Figure 9: Samsung S8 Kalman Filtered Doppler RMS

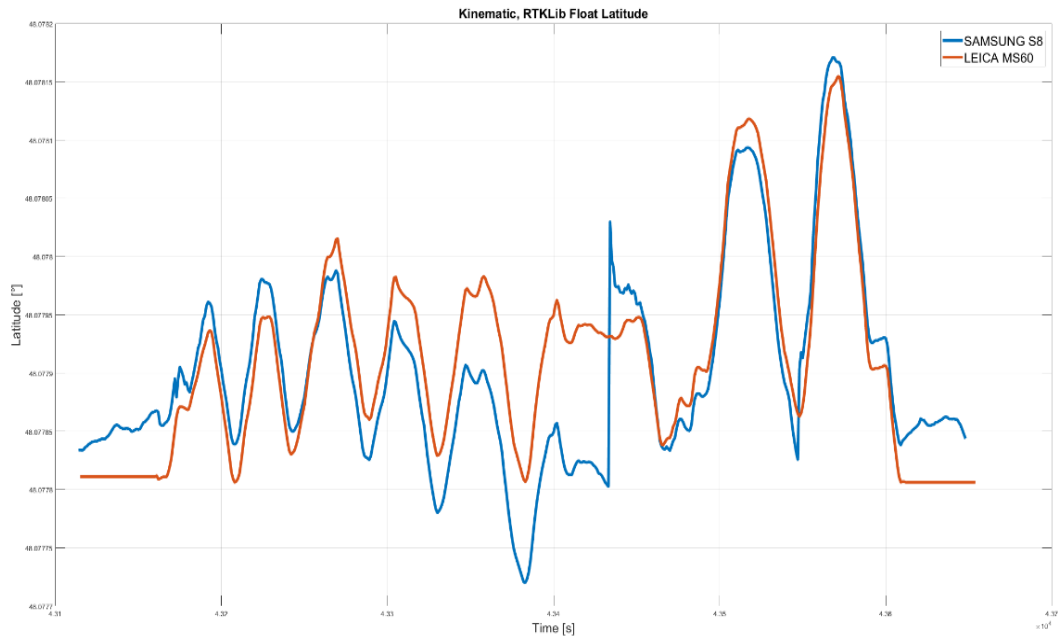


Figure 10: Samsung S8 RTK Float Solution w.r.t Reference System

Furthermore, the investigation was carried out on the code and carrier phase residual. The code range residuals as expected are very noisy (average of 15 meters) in comparison to carrier residual. The carrier residual experiences sudden rise due to cycle slips. The integrated RTKLib was used to perform RTK positioning. In the preliminary investigation, it was found that the RTKLib filters out more than 80 percent of the pseudorange resulting into invalid solution. The solution validation test (chi-squared test) is included in the RTKLib to exclude invalid solutions due to unmodeled measurement errors [1].

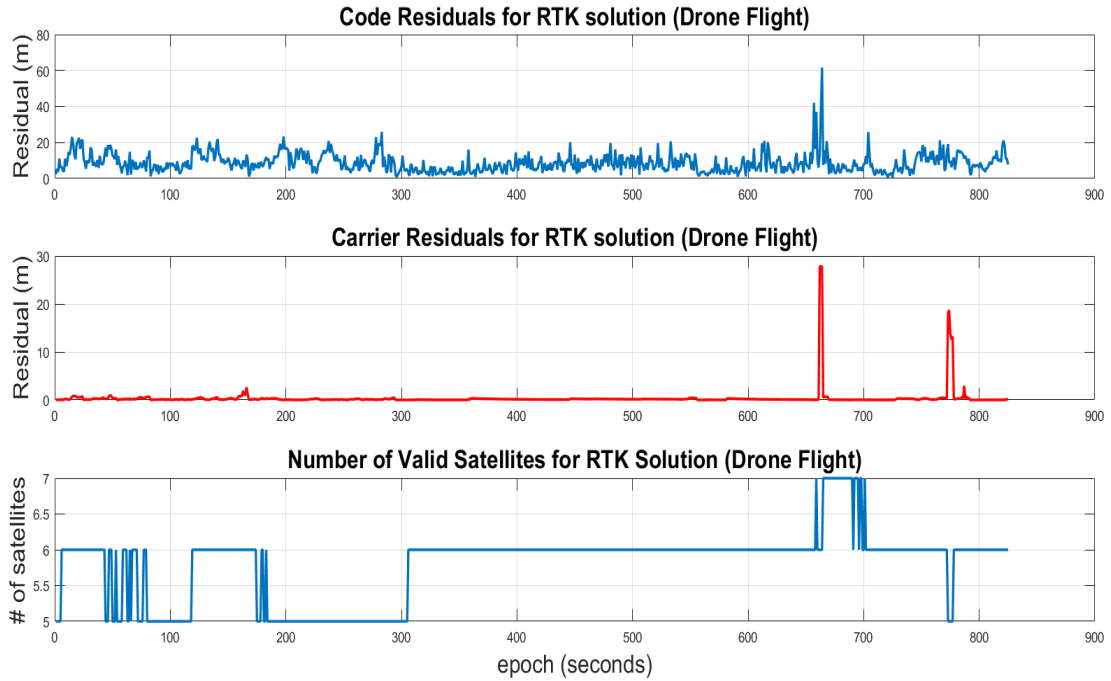


Figure 11: Raw Data Analysis from S8 during Drone Flight

Thus, bypassing the solution validation test allows larger epoch pseudoranges to be processed by the RTKLib. But, results in wrong ambiguity fixing. The ambiguity resolution ratio threshold was set to 3 and as can be seen that for few epoch the ambiguity resolution ratio exceeds the threshold value but the positioning accuracy is quite absurd.

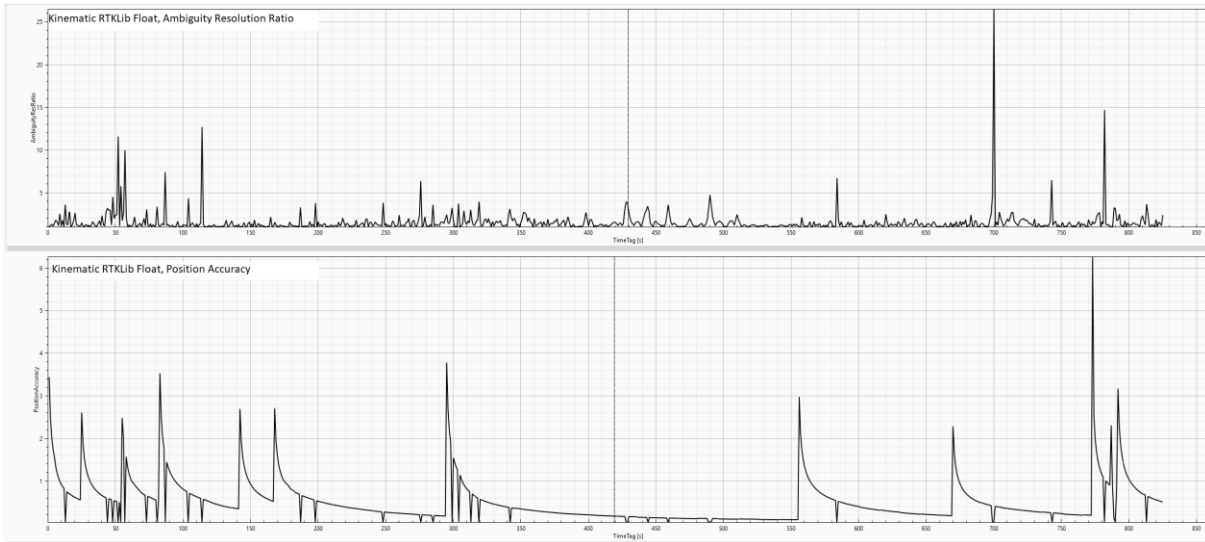


Figure 12: Ambiguity Resolution Ratio and Position Accuracy for RTK Float Solution during Drone Flight

STATIC RETRANSMISSION ANALYSIS

Figure 13 depicts the SNR for all the satellites in the static retransmission scenario. GPS only is used, for which 5 satellites with a SNR of 35 dB-Hz or higher are present throughout the whole measurement.



Figure 13: SNR plot for the static retransmission scenario

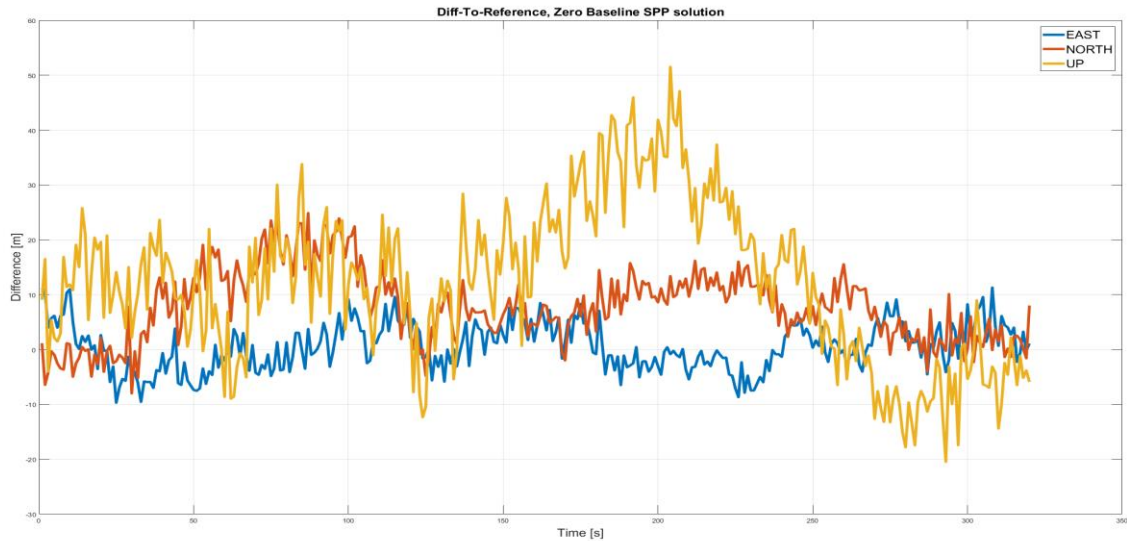


Figure 14: Static retransmission, SPP solution

Figure 14 shows the SPP results for the static retransmission scenario. The difference w.r.t. the reference position reaches up to 55m (UP component). The overall position solution is extremely noisy with no visible overlying drift. The variations in the horizontal

component regarding the reference position are mainly contained within a +/- 10m interval. The positioning results are within the expected scope of what can be deferred from the kinematic scenario.

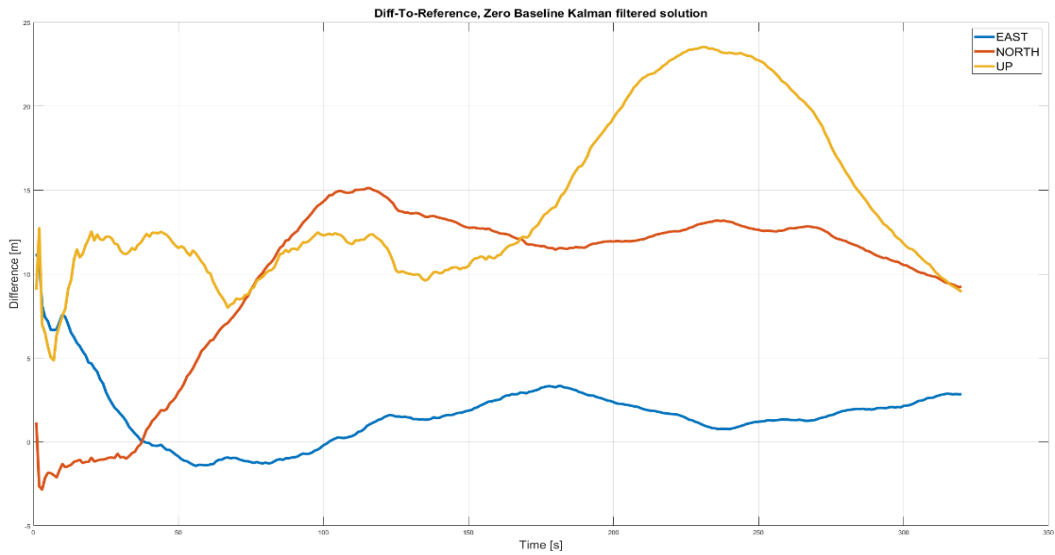


Figure 15: Static retransmission scenario, Kalman filtered solution

The Kalman filtered SPP solution (Figure 15) shows as in the previous experiment a large improvement of position consistency and deviation. The maximum difference to the reference position is decreased by approximately 30 meters (from ~55m to ~25m) and deviations in all 3 components start to converge close to zero (around 5 meters of difference to reference). Keep in mind, compared to the kinematic ones those results are not demeaned, hence this offset to zero respective all the differences to the reference position contain atmospheric effects. The reason only the first five minutes of this dataset are illustrated can be derived from Figure 16 and Figure 17.

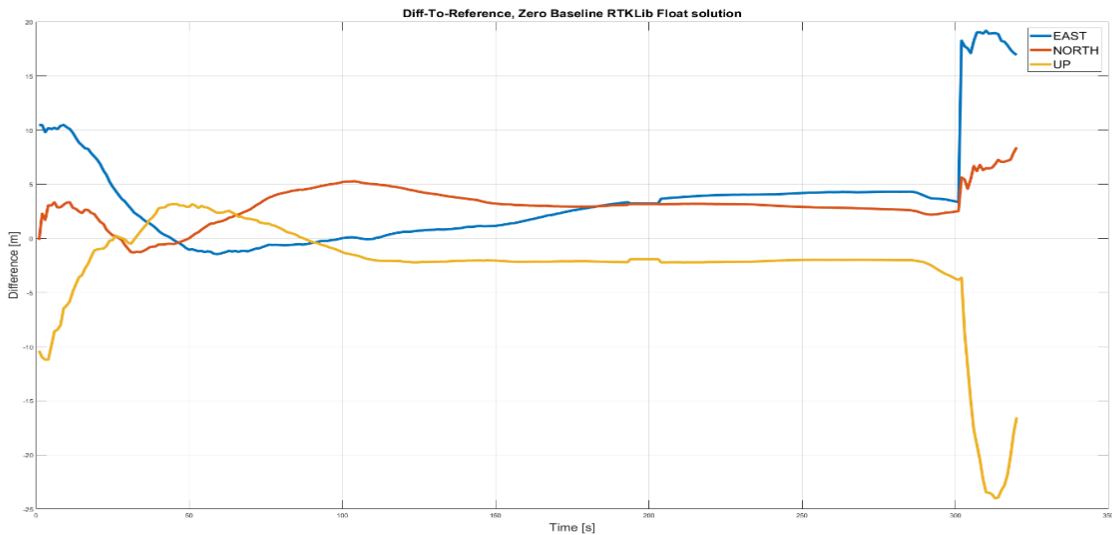


Figure 16: Static retransmission scenario, RTKLib float solution

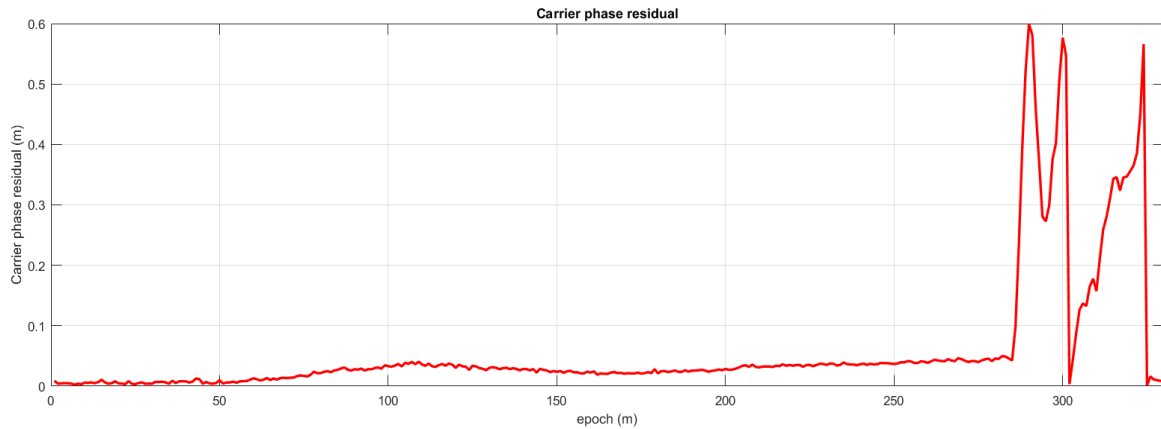


Figure 17: Static retransmission scenario, carrier phase residuals

The dataset is continuous until approximately minute 4:30, then several cycle slips occur. After these incidents the RTK filter is no longer able to maintain its very smooth trajectory (Figure 16), which, up to this point, performed very well (compared to the other solutions) with all three coordinate components steadily below a difference of five meters with respect to the reference coordinates. Taking into account Figure 18, the first cycle slip at around second 280 caused the solution of the filter to drift away.

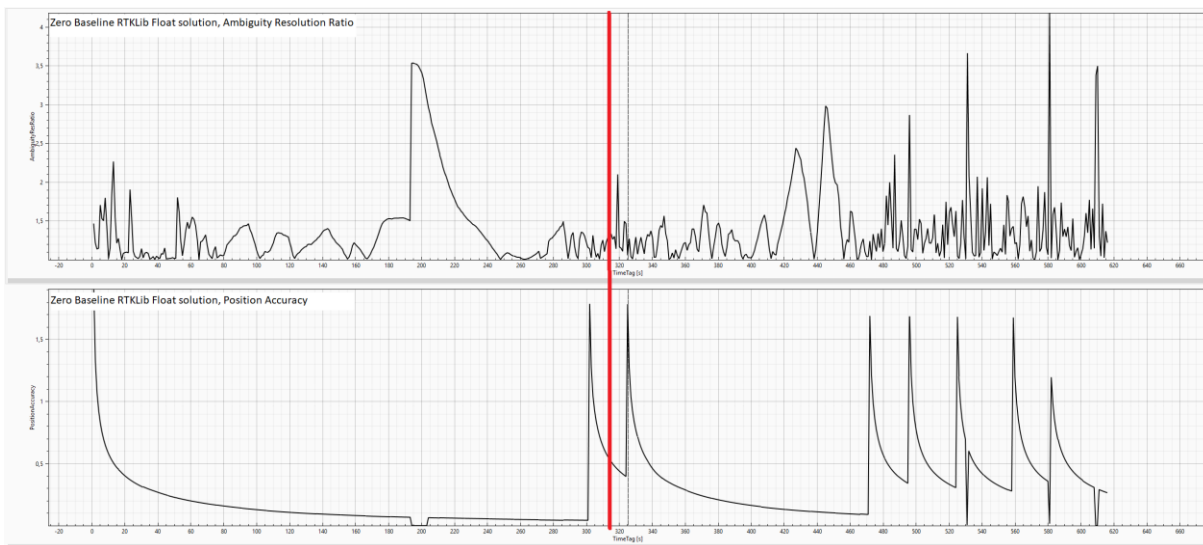


Figure 18: RTKLib float solution, ambiguity resolution ratio and position accuracy

At this point the assumed position accuracy of the filter is uncompromised, which leads the filter to believe the solution is still accurate, hence the position starting to drift away (Figure 16). With the additional cycle slip at second 305 finally the position accuracy is reset and the position accuracy is reevaluated, hence allowing the filter to rescale its error measures and admit larger discontinuities in the solution.

Using LMSOft, a tool to analyze especially bad GNSS data, only GPS L1 carrier phase data was analyzed. During the preprocessing (data snooping) the software detected cycle slips for each satellite and each epoch, which are common to all satellites. Similar to code measurements, these incidents can be treated as “carrier clock jumps”, and, using the LMSOft float RTK filter, when only using the double difference cycle slip detector and deactivating the single channel cycle slip detector, the filter converges and carrier phase residuals drop below the 5mm level, making them useful for precise positioning and RTK processing.

FEASIBILITY OF INS INTEGRATION

Now for the INS to be able to support the position solution in terms of stability and accuracy the IMU needs to be able to properly detect the motion of the rover to correct for cycle slips between the single measurement epochs. This implies though, that the single sensors' stability with respect to drift, mainly the gyroscope, and the noise level need to be sufficiently low. Speaking in absolute terms, the position error introduced by the gyroscope drift and noise need to be lower than half the wavelength of the carrier's signal which is used for positioning. The error in the respective axis Δx can be calculated using

$$\Delta x = \frac{1}{6} * (\Delta t)^3 * g * G$$

Where, Δt is the time interval (1 second), $g = 9.81 \frac{m}{s^2}$ and G is the gyroscope bias instability obtained from the Allan-Variance evaluation depicted in Figure 19.

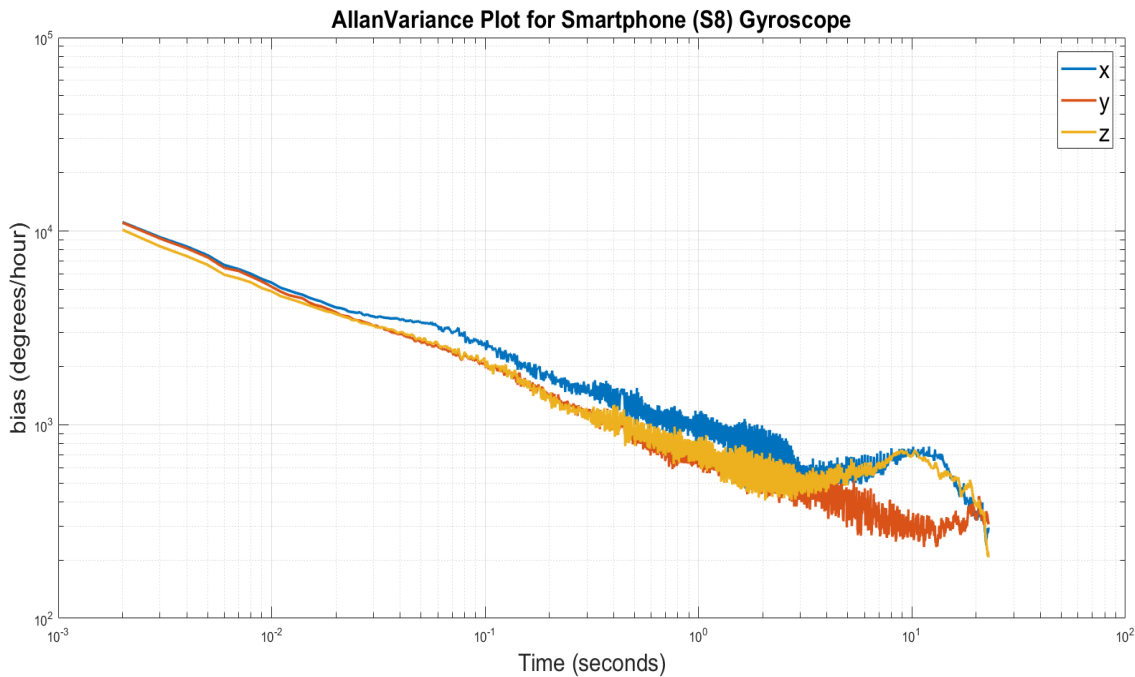


Figure 19: Allan Variance for Samsung S8 gyroscopes

With $G_x = 0.0023$ rad/sec and $G_y = 0.0011$ rad/sec the position error due to the gyroscope bias instability then yields $\Delta x = 0.0036m$ and $\Delta y = 0.0032m$ (the values for G were reached at an integration time of 1.66s and 4.09s for x and y respectively). This is still way below the L1 wavelength of approximately $0.19m$. Using precise error models for the IMU will allow for shorter integration times with a comparable accuracy, hence enabling a deep coupling of the inertial sensor with the smartphone GNSS.

CONCLUSION

Regarding the kinematic scenario, a simple SPP solution is not sufficient. The measurements are too inaccurate, too noisy, only the very coarse progression of the trajectory can be extracted. Small movements are undetectable. By exploiting the Doppler measurements a smoothed trajectory is filtered, yielding the most promising results of the overall comparison. Performing RTK by using the open source RTKLib was only possible after adjusting the RTKLib code residual filtering, allowing all measurements to the RTK processing. Hence, the solution becomes more robust but very less precise, losing its potential advantage over the Doppler Smoothed Pseudorange solution.

For the static retransmission scenario again the SPP solution performed worst. However this time, by exploiting an advantageous measurement setup yielding relatively consistent data, the RTK float solution became very stable until cycle slips occurred,

outperforming the Doppler Smoothed solution. The float position was maintained with respect to the reference coordinates within 3 meters until signal loss.

The raw carrier phase provided by the phone is of moderate quality. The carrier phase residuals may range up to 10 centimeters and "Duty Cycling" is a major drawback for precise carrier phase positioning. Additional analysis however shows, that by only using a double difference cycle slip detector and estimating the clock error and carrier phase ambiguities for an unknown but static rover, the filter converges. In this very case, the double difference preprocessor detects cycle slips every epoch, which are common to all satellites. They can be interpreted as a "carrier clock jump". The results presented in the research are the preliminary analysis on the feasibility of RTK positioning using GNSS raw from the mobile phone. The research shows that the direct RTK processing is not feasible without the exclusion of solution validation, which in results deteriorate the accuracy of RTK positioning. However, we are quite certain that the identified issues can be resolved.

Finally, supporting the GNSS solution by the inbuilt IMU seems feasible regarding the accuracy of the IMU. The position error due to gyroscope bias instability is below the L1 wavelength, allowing the usage of those measurements for a cycle slip detection given a GNSS/INS integration with sensor error model and estimation.

ACKNOWLEDGMENTS

We would like to express our deepest regards to Prof. Dr. Thomas Pany for his guidance and Mr. Daniel Maier for managing the drone flight for the test setup.

REFERENCES

- [1] T. Takasu, "RTKLIB: An Open Source Program Package for GNSS Positioning," [Online]. Available: <http://www.rtklib.com/>.